Modified Kirchhoff Diffraction of Pulsed EM Waves Radiated from a Slot-Excited Fabry-Perot Resonator Antenna

Stumpf, Martin; Lager, Ioan E.; Vandenbosch, Guy A.E.

DOI
10.1049/cp.2018.0447

Publication date
2018

Document Version
Final published version

Published in
Proceedings - 12th European Conference on Antennas and Propagation, EUCAP 2018

Modified Kirchhoff Diffraction of Pulsed EM Waves Radiated from a Slot-Excited Fabry-Pérot Resonator Antenna

Martin Štumpf
SIX Research Centre
Brno University of Technology
Technická 3082/12,
616 00 Brno, the Czech Republic
Email: martin.stumpf@centrum.cz

Guy A. E. Vandenbosch
Electrical Engineering Dpt., TELEMIC
Katholieke Universiteit Leuven
Kasteelpark Arenberg 10 bus 2444
B-3001 Leuven, Belgium
Email: guy.vandenbosch@kuleuven.be

Ioan E. Lager
Faculty of Electrical Engineering,
Mathematics and Computer Science
Delft University of Technology
Mekelweg 4,
2628 CD Delft, the Netherlands
Email: i.e.lager@tudelft.nl

***Abstract*—Diffraction of pulsed electromagnetic (EM) waves in a slot excited Fabry Perót type resonator antenna is studied analytically in the modified Kirchhoff approximation. Closed-form space-time expressions for the radiated EM fields are found using the Cagniard-DeHoop technique. Illustrative numerical examples are given.**

I. Introduction

Fabry Perót (FP) antennas continue to capture the attention of researchers, as demonstrated by the recent publications [1]–[3]. This attention is justified by the unique operational opportunities offered by the radiation from FP cavities (and the largely similar leaky-wave radiation): high-gain and low profile [1], [3]–[5], and ultra-wide band (UWB) performance combined with very low dispersion [6]. FP antennas serve applications ranging from wide-deployment, low-cost ones, such as WLAN [2], up to high-end, sophisticated astronomical instrumentation systems [7], their all-encompassing capability being suggestively covered in [8].

The all-around electromagnetic (EM) radiation serviceability of FP cavities has a long history, with [9] discussing the gain enhancement in the microwave regime and [10] the design of masers operating at infrared and optical frequencies. Their operational attractiveness fueled intense research into their modeling and analysis. Early studies comprised iterative approaches that were called upon whenever a corresponding scalar approximation was applicable [11], or via the modified Kirchhoff approximation [12]. Increasingly elaborate and computationally efficient techniques were required as modeling and analysis was embedded in design and optimization strategies. It is interesting to note that, to the authors' best knowledge, the analysis of FP antennas was always done in the frequency-domain (FD), a typical example being [13] that applied a FD, ray theory approximation. Even recently, the FD analysis remains the tool of choice despite UWB operation being often the main design objective [6], [8].

The assessment of UWB and dispersion performance is more effectively carried out in the time-domain (TD). This approach is missing in literature and the present paper will fill this gap. The main investigation instrument to this end will be he *Cagniard-DeHoop* (CdH) technique, a sophisticated mathematical tool for analyzing TD wave field propagation in stratified media [14], [15]. The method has been recently shown to accurately and computationally effectively describe the pulsed EM-field radiation from various slot-antenna configurations [16]–[19]. Furthermore, transient wave field diffraction by a semi-infinite screen can be solved analytically with the aid of a combination of the Wiener-Hopf and CdH technique [20], [21]. The same approach was also proved to successfully tackle the analysis of configurations involving the interface of two dielectric half-spaces [22] and for handling multiple wave reflections [23], [24]. In the case of configurations where a planar obstacle of bounded extent is present, an approach based on the (modified) Kirchhoff approximation may reveal interesting closed-form TD analytical results [25]. Their striking simplicity renders them extremely favorable for being included in antenna design optimization schemes. Moreover, the modeling accuracy recommends this approach for EM compatibility (EMC) studies, both theoretically and in measurement protocols where the UWB, low-dispersivity FP antennas can play a decisive role.

The account now proceeds by the problem definition, followed by a (brief) outlining of the steps that are required for obtaining the solution. The method's potential will be demonstrated by means of some illustrative numerical experiments after which conclusions will be drawn.

II. Problem definition

The problem configuration under consideration is shown in Fig. 1. The FP antenna consists of a narrow exciting slot and a PEC screen placed in above the slot. The antenna radiates pulsed EM waves into the unbounded half-space, $x_3 > 0$, where these waves are diffracted by the PEC screen occupying a domain $\Sigma = \{-\ell/2 \leq x_1 \leq \ell/2, x_3 = h\}$. The EM properties of the surrounding half-space are described by (real-valued and positive) permittivity ϵ_0 and permeability μ_0. The corresponding EM wave speed is $c_0 = (\epsilon_0\mu_0)^{-1/2} > 0$ and $\eta_0 = (\epsilon_0/\mu_0)^{1/2} > 0$ denotes the free-space wave admittance.

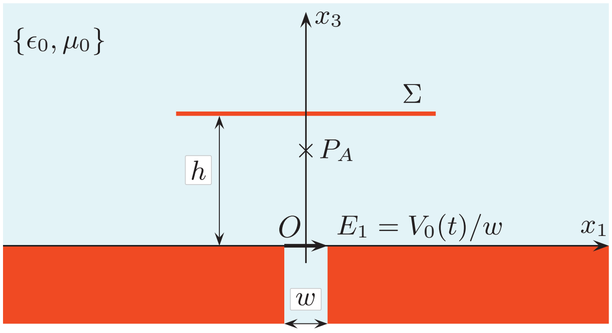

Fig. 1. A Fabry-Perot slot-excited resonator antenna.

Partial differentiation with respect to x_κ is denoted by ∂_κ with $\kappa = 1$ or $\kappa = 3$; the differentiation with respect to time is ∂_t. The Heaviside unit step function is denoted by $\mathrm{H}(t)$ and the Dirac delta distribution is $\delta(t)$.

III. Problem Formulation

The radiated EM-field fields do satisfy the EM field equations [26, Sec. 18.2]

$$\partial_1 H_2 - \epsilon_0 \partial_t E_3 = 0 \tag{1}$$

$$\partial_3 H_2 + \epsilon_0 \partial_t E_1 = 0 \tag{2}$$

$$\partial_1 E_3 - \partial_3 E_1 - \mu_0 \partial_t H_2 = 0 \tag{3}$$

that are supplemented with the excitation condition

$$\lim_{x_3 \downarrow 0} E_1(x_1, x_3, t) = V_0(t)\delta(x_1) \tag{4}$$

as $w \downarrow 0$, for all $x_1 \in \mathbb{R}$ and all $t > 0$ and with the continuity condition

$$\lim_{x_3 \downarrow h} E_1(x_1, x_3, t) - \lim_{x_3 \uparrow h} E_1(x_1, x_3, t) = 0 \tag{5}$$

and the jump condition across the screen Σ

$$\begin{aligned} &\lim_{x_3 \downarrow h} H_2(x_1, x_3, t) - \lim_{x_3 \uparrow h} H_2(x_1, x_3, t) \\ &\quad = -2\eta_0 \sum_{n=1}^{\infty} V_0[t - (2n-1)h/c_0] \\ &\qquad [\mathrm{H}(x_1 + \ell/2) - \mathrm{H}(x_1 - \ell/2)]/\ell \end{aligned} \tag{6}$$

for all $x_1 \in \mathbb{R}$ and all $t > 0$, where $V_0(t)$ is the excitation gap voltage pulse. The Kirchhoff-approximate jump condition results from an x_1-independent wave motion that consists of successively reflected uniform plane waves confined between the PEC planes in the finite interval $\{-\ell/2 \leq x_1 \leq \ell/2\}$ extending over the PEC screen. Finally, it is assumed that the EM wave fields are activated at $t = 0$ and that prior to this instant these fields are zero throughout the problem configuration.

IV. Transform-Domain Solution

The problem formulated in the previous section can be solved with the aid of the CdH technique [14]. This technique employs a one-sided Laplace transformation with respect to time with the *positive and real-valued* transform parameter, which parameter is used as a scaling parameter in the wave slowness representation taken in the direction parallel to the planar interface. The representation is subsequently cast into an integral that is recognized as the Laplace transformation. Relying on the Lerch uniqueness theorem of the one-sided Laplace transformation, the desired TD result is finally found upon inspection. The space-time expressions given in the following section have been found exactly along these lines.

V. Space-Time Solution

The incident wave field corresponds to the fundamental solution of the 2D wave equation, i.e.

$$H_2^{\mathrm{i}}(x_1, x_3, t) = \frac{\epsilon_0}{\pi}\partial_t V_0(t) *_t \frac{\mathrm{H}(t - r/c_0)}{(t^2 - r^2/c_0^2)^{1/2}} \tag{7}$$

for all $x_1 \in \mathbb{R}$, $\{x_3 \in \mathbb{R}; x_3 > 0\}$ and all $\{t \in \mathbb{R}; t > 0\}$. Here, $r = (x_1^2 + x_3^2)^{1/2} > 0$ is the distance from the radiating slot. The remaining Kirchhoff-diffracted-wave constituents can be described as

$$\begin{aligned} &H_2^{\mathrm{d};n}(x_1, x_3, t) = \eta_0 \big\{V_0[t - (x_3 + 2nh)/c_0] \\ &+ V_0[t - (2nh - x_3)/c_0]\big\}[\mathrm{H}(x_1 + \ell/2) - \mathrm{H}(x_1 - \ell/2)]/\ell \\ &+ \delta[t - (2n-1)h/c_0] *_t [\eta_0 V_0(t)/\ell] \\ &*_t \frac{1}{\pi}\left\{ \frac{(x_1 - \ell/2)(x_3 + d)}{c_0^2 t^2 - (x_3 + d)^2} \frac{\mathrm{H}(t - T_{\mathrm{R}+})}{(t^2 - T_{\mathrm{R}+}^2)^{1/2}} \right. \\ &- \frac{(x_1 + \ell/2)(x_3 + d)}{c_0^2 t^2 - (x_3 + d)^2} \frac{\mathrm{H}(t - T_{\mathrm{L}+})}{(t^2 - T_{\mathrm{L}+}^2)^{1/2}} \\ &+ \frac{(x_1 - \ell/2)(d - x_3)}{c_0^2 t^2 - (d - x_3)^2} \frac{\mathrm{H}(t - T_{\mathrm{R}-})}{(t^2 - T_{\mathrm{R}-}^2)^{1/2}} \\ &\left. - \frac{(x_1 + \ell/2)(d - x_3)}{c_0^2 t^2 - (d - x_3)^2} \frac{\mathrm{H}(t - T_{\mathrm{L}-})}{(t^2 - T_{\mathrm{L}-}^2)^{1/2}} \right\} \end{aligned} \tag{8}$$

for the diffracted field below the PEC screen, where

$$T_{\mathrm{R}+} = [(x_1 - \ell/2)^2 + (x_3 + d)^2]^{1/2}/c_0 \tag{9}$$

$$T_{\mathrm{L}+} = [(x_1 + \ell/2)^2 + (x_3 + d)^2]^{1/2}/c_0 \tag{10}$$

$$T_{\mathrm{R}-} = [(x_1 - \ell/2)^2 + (d - x_3)^2]^{1/2}/c_0 \tag{11}$$

$$T_{\mathrm{L}-} = [(x_1 + \ell/2)^2 + (d - x_3)^2]^{1/2}/c_0 \tag{12}$$

are the arrival times of the cylindrical wavefronts. A similar expression applies to the diffracted field above the screen. Finally, the total wave field is found as

$$H_2 = H_2^{\mathrm{i}} + \sum_{n=1}^{\infty} H_2^{\mathrm{d};n} \tag{13}$$

In virtue of causality, the total number of the diffracted-wave terms $H_2^{\mathrm{d};n}$ is always finite in any bounded time window of observation.

VI. Numerical examples

The obtained space-time expressions have been implemented in Matlab®. In the following numerical examples, the PEC screen of length ℓ is placed above the narrow slot at height $h = \ell$. The excitation gap voltage is described by:

- *The power-exponential (PE) pulse* [27], [28]

$$V_0(t) = V_{\rm m}\,(t/t_{\rm r})^{\nu}\exp[-\nu(t/t_{\rm r}-1)]\,{\rm H}(t) \qquad (14)$$

  where $V_{\rm m}$ is the pulse amplitude, $t_{\rm r}$ is the pulse rise time and $\nu > 0$ is the rising exponent. The pulse time width $t_{\rm w}$ is then related to $t_{\rm r}$ and ν via $t_{\rm w} = t_{\rm r}\nu^{-\nu-1}\Gamma(\nu+1)\exp(\nu)$, where $\Gamma(x)$ is the Euler gamma function. Here, we take $V_{\rm m} = 1.0\,({\rm V})$, $\nu = 2$ and $c_0 t_{\rm w} = 0.20\,\ell$.

- *The windowed-power (WP) pulse* [29]

$$V_0(t) = V_{\rm m}\,(t/t_{\rm r})^{\nu}\,[2-(t/t_{\rm r})]^{\nu}\,{\rm H}(t){\rm H}(2t_{\rm r}-t) \qquad (15)$$

  where the intervening parameters being the same as in (14). Unlike the PEpulse, whose tail extends indefinitely, the WPis time-windowed, its time width being $2t_{\rm r}$.

In our experiments, we take $V_{\rm m} = 1.0\,({\rm V})$, $\nu = 2$ and $c_0 t_{\rm w} = 0.20\,\ell$. The entailed pulse time width is chosen such that particular reflected-wave constituents can be clearly distinguished. The excitation pulse shapes are shown in Fig. 2.

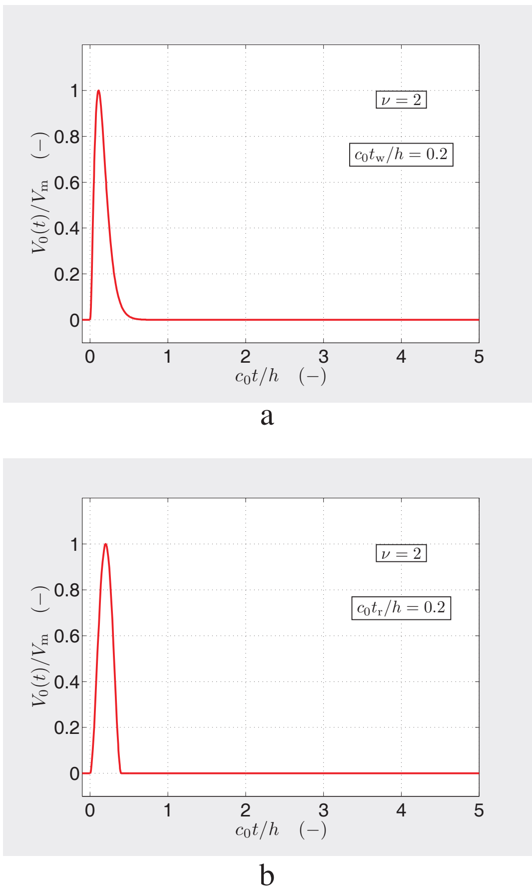

Fig. 2. Excitation pulse shape. (a) Unipolar PE pulse; (b) unipolar WP pulse.

The spatial distribution of the magnetic field in the spatial window of observation $\{-\ell \le x_1 \le \ell, 0 \le x_3 \le 2\ell\}$ and at time points $c_0 t = \{1.0h, 1.50h\}$ is firstly examined, the results being shown in Fig. 3 for the PE excitation and in Fig. 4 for the WP excitation.

- Figures 3(a) and 4(a) illustrate the field distribution at $c_0 t = h = \ell$, when the wavefront hits the PEC screen. Up to that instant, the total field is identical to the incident wave field given in Eq. (7). As an interesting detail, because of H_2 being related to the time convolution of the *time derivative* of the exciting voltage pulse with the 2D Green's function (see Eqs. (7) and (8)), the wavefront reflects the signature of the excitations' time derivative, with the characteristic symmetric shape in the case of the WP excitation (see [29, Fig. 2]).
- Figures 3(b) and 4(b) evidence the complex field distribution that has shaped up shortly upon passing the PEC obstacle. Here, the downgoing reflected and upgoing transmitted wave constituents are clearly distinguishable. Later, after the leading wavefront propagates out of the chosen spatial window of observation, the field is still partly trapped via its reflections against the PEC planes. It should be noted that, although the WP excitation is time-windowed, the total radiated wave field *does not have a finite support* due to the 2D Green's function with an infinitely long tail.

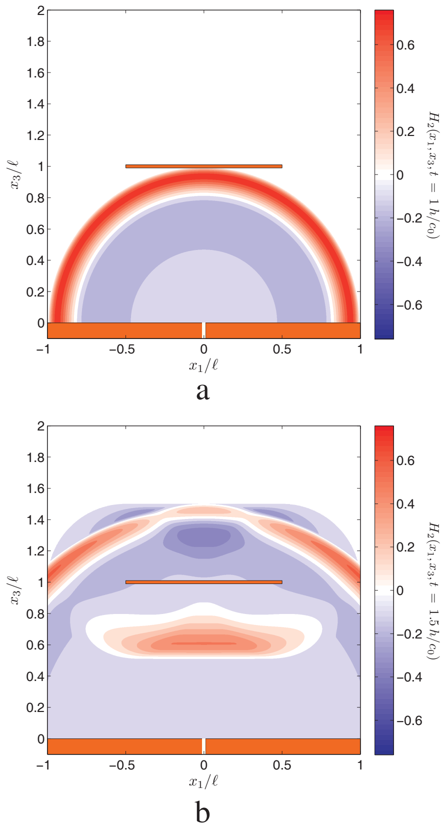

Fig. 3. The magnetic-field spatial distribution observed at (a) $c_0 t = 1.00h$ and (b) $c_0 t = 1.50h$ – PE excitation.

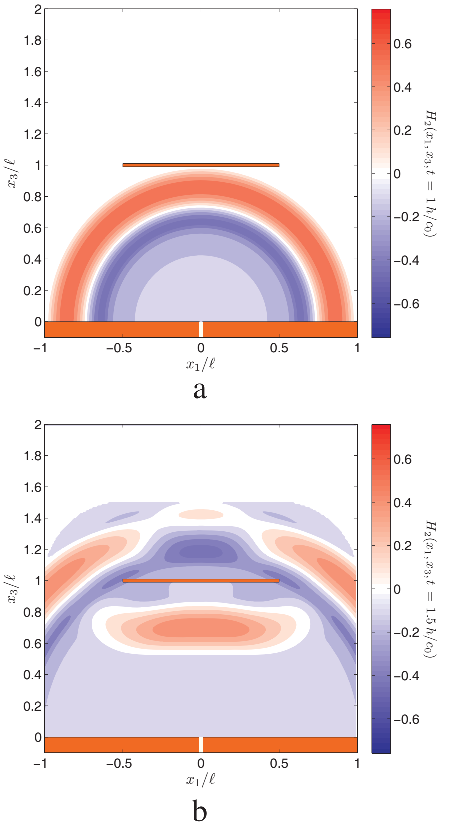

Fig. 4. The magnetic-field spatial distribution observed at (a) $c_0 t = 1.00h$ and (b) $c_0 t = 1.50h$ – WP excitation.

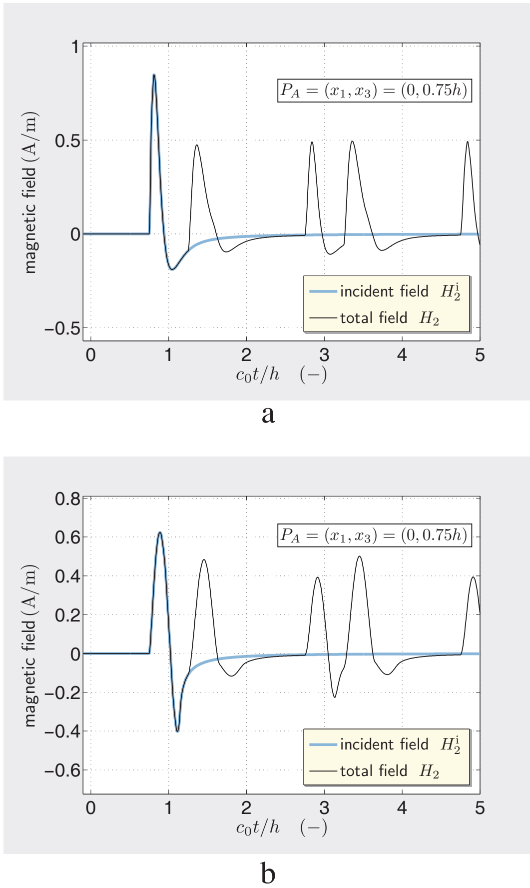

Fig. 5. Incident and total field signatures at $P_A = (x_1, x_3) = (0, 0.75h)$ (see Fig. 1). (a) PE excitation; (b) WP excitation.

The intricate temporal behaviour of the field in between the radiator and the PEC screen is further demonstrated by the signatures in Fig. 5. Apart from the expected multiple reflections, these plots also illustrate, once again, the differences between the two employed pulse shapes.

VII. Conclusions

The time-domain, analytical modeling of the pulsed EM wave diffraction in a slot excited Fabry Perót type resonator antenna via the modified Kirchhoff approximation was demonstrated. Closed-form space-time expressions for the radiated EM fields were arrived at by using the Cagniard-DeHoop technique. The method's performance was illustrated via representative numerical experiments concerning both infinitely extended and time-windowed excitations.

Acknowledgment

The research reported in this paper was financed by the Czech Science Foundation under Grant 17-05445Y and supported in part by the Czech Ministry of Education, Youth and Sports under Grant LO1401 [the National Sustainability Program].

This paper is dedicated to Professor Adrianus T. de Hoop on the occasion of his 90$^{\text{th}}$ *aniversary. The authors wish to express hereby their entire gratitude for the constant inspiration and encouragement that they received over many years.*

References

[1] R. Guzmán-Quirós, A. R. Weily, J. L. Gómez-Tornero, and Y. J. Guo, "A Fabry Perót antennawith two-dimensional electronic beam scanning," *IEEE Trans. Antennas Propag.*, vol. 64, no. 4, pp. 1536–1541, Apr. 2016.

[2] M. L. Abdelghani, H. Attia, and T. A. Denidni, Dual- and wideband Fabry Perót resonator antenna for WLAN applications," *IEEE Antennas Wireless Propag. Lett.* vol. 16, pp. 473–476, Aug. 2017.

[3] A. K. Singh, M. P. Abegaonkar, and S. K. Koul, "High-gain and high-aperture-efficiency cavity resonator antenna using metamaterial superstrate," *IEEE Antennas Wireless Propag. Lett.* vol. 16, pp. 2388–2391, Aug. 2017.

[4] A. P. Feresidis, G. Goussetis, S. Wang, and J. C. Vardaxoglou, "Artificial magnetic conductor surfaces and their application to low-profile high-gain planar antennas," *IEEE Trans. Antennas Propag.*, vol. 53, no. 1, pp. 209–215, Jan. 2005.

[5] A. R. Weily, T. S. Bird, and Y. J. Guo, "A reconfigurable high-gain partially reflecting surface antenna," *IEEE Trans. Antennas Propag.*, vol. 56, no. 11, pp. 3382–3390, Nov. 2008.

[6] A. Neto, "UWB, non dispersive radiation from the planarly fed Leaky Lens Antenna – Part 1: Theory and design," *IEEE Trans. Antennas Propag.*, vol. 58, no. 7, pp. 2238–2247, Jul. 2010.

[7] D. Burghoff, T.-Y. Kao, N. Han, C. W. I. Chan, X. Cai, Y. Yang, D. J. Hayton, J.-R. Gao, J. L. Reno, and Q. Hu, "Terahertz laser frequency combs," *Nature Photonics*, vol. 8, pp. 462–467, Jun. 2014. [Online]. doi:10.1038/NPHOTON.2014.85.

[8] D. R. Jackson, P. Burghignoli, G. Lovat, F. Capolino, J. Chen, D. R. Wilton, and A. A. Oliner, "The fundamental physics of directive beaming at microwave and optical frequencies and the role of leakywaves," *Proc. IEEE*, vol. 99, no. 10, pp. 1780–1805, Oct. 2011.

[9] G. V. Trentini, "Partially reflecting sheet arrays," *IRE Trans. Antennas Propag.*, vol. 4, no. 4, pp. 666–671, Oct. 1956.

[10] A. L. Schawlow and C. H. Townes, "Infrared and optical masers," *Phys. Rev.*, vol. 112, no. 6, p. 1940, Dec. 1958.

[11] A. G. Fox and T. Li, "Resonant modes in a maser interferometer," *Bell Labs Tech. J.*, vol. 40, no. 2, pp. 453–488, Mar. 1961.

[12] H. Blok, *Diffraction theory of open resonators*, Ph.D. dissertation, Delft University of Technology, Delft, the Netherlands, 1970.

[13] A. P. Feresidis and J. Vardaxoglou, "High gain planar antenna using optimised partially reflective surfaces," *IEE Proc.-Microw. Antennas Propag.*, vol. 148, no. 6, pp. 345–350, Dec. 2001.

[14] A. T. De Hoop, "A modification of Cagniard's method for solving seismic pulse problems," *Appl. Sci. Res., Sec. B*, vol. 8, no. 1, pp. 349–356, Dec. 1960.

[15] M. Štumpf, A. T. De Hoop, and G. A. Vandenbosch, "Generalized ray theory for time-domain electromagnetic fields in horizontally layered media," *IEEE Trans. Ant. Propag.*, vol. 61, no. 5, pp. 2676–2687, May 2013.

[16] M. Štumpf, A. T. De Hoop, and I. E. Lager, "Pulsed electromagnetic field radiation from a narrow slot antenna with a dielectric layer," *Radio Sci.*, vol. 45, no. 5, Oct. 2010.

[17] M. Štumpf, A. T. De Hoop, and I. E. Lager, "Closed-form time-domain expressions for the 2D pulsed EM field radiated by an array of slot antennas of finite width," in *Proc. 2010 URSI Int. Symp. Electromagnetic Theory*, Berlin, Germany, 2010, pp. 703–706.

[18] A. T. De Hoop, M. Štumpf, and I. E. Lager, "Pulsed electromagnetic field radiation from a wide slot antenna with a dielectric layer," *IEEE Trans. Ant. Propag.*, vol. 59, no. 8, pp. 2789–2798, Aug. 2011.

[19] M. Štumpf and Z. Raida, "Pulsed electromagnetic waves between parallel plates: The modal-expansion and generalized-ray approaches," *IEEE Ant. Propag. Mag.*, vol. 56, no. 6, pp. 90–101, Dec. 2014.

[20] A. T. De Hoop, "Representation theorems for the displacement in an elastic solid and their application to elastodynamic diffraction theory," Ph.D. dissertation, Delft University of Technology, Delft, the Netherlands, 1958.

[21] A. T. De Hoop and M. V. De Hoop, "Transient elastic P and SV wave edge diffraction by a semi-infinite perfect-slip fracture in an isotropic dispersive solid: a canonical problem," *J. Geophys. Res.*, vol. 108, no. B4, Apr. 2003.

[22] R. Du Cloux, "Pulsed electromagnetic radiation from a line source in the presence of a semi-infinite screen in the plane interface of two different media," *Wave Motion*, vol. 6, no. 5, pp. 459–476, Sep. 1984.

[23] B. J. Kooij and D. Quak, "Three-dimensional scattering of impulsive acoustic waves by a semi-infinite crack in the plane interface of a half-space and a layer," *J. Math. Phys.*, vol. 29, no. 7, pp. 1712–1721, Jul. 1988.

[24] K. F. Haak and B. J. Kooij, "Transient acoustic diffraction in a fluid layer," *Wave Motion*, vol. 23, no. 2, pp. 139–164, 1996.

[25] A. T. De Hoop, "Transient two-dimensional Kirchhoff diffraction of a plane elastic SH wave by a generalized linear-slip fracture," *Geophys. J. Int.*, vol. 143, no. 2, pp. 319–327, Nov. 2000.

[26] A. T. De Hoop, *Handbook of Radiation and Scattering of Waves*, London, UK: Academic Press, 1995.

[27] D. Quak, "Analysis of transient radiation of a (traveling) current pulse on a straight wire segment," in *Proc. 2001 IEEE Int. Symp. on Electromagnetic Compat.*, Montreal, Que., Canada, Jul. 2001, pp. 849–854.

[28] I. E. Lager, A. T. de Hoop, and T. Kikkawa, "Model pulses for performance prediction of digital microlectronic systems," *IEEE Trans. Compon., Packag., Manuf. Technol.*, vol. 2, no. 11, pp. 1859–1870, Nov. 2012.

[29] I. E. Lager and S. L. van Berkel, "Finite temporal support pulses for EM excitation," *IEEE Antennas Wireless Propag. Lett.* vol. 16, pp. 1659–1662, Jun. 2017.